Formulation of Stochastic MPC to Balance Intermittent Solar Power with Hydro Power in Microgrid

Madhusudhan Pandey, Dietmar Winkler, Roshan Sharma, Bernt Lie*

TMCC, University of South-Eastern Norway, Bernt.Lie@usn.no

Abstract

In a microgrid with both intermittent and dispatchable generation, the intermittency caused by sources such as solar power and wind power can be balanced using dispatchable sources like hydro power. Both generation and consumption are stochastic in nature and require future prediction. The stochasticity of both generation and consumption will drift the grid frequency. Improved performance of the grid can be achieved if the operation of the microgrid is optimized over some horizon, for instance formulating Model Predictive Control (MPC), with the added problem that intermittent sources vary randomly into the future. In this paper, first, we have formulated a deterministic MPC and compared it with a PI controller. Second, a stochastic MPC (SMPC) based on a multi-objective optimization (MOO) scheme is presented. Results from deterministic MPC show that the overall performance of MPC is better than the PI controller for dispatching the required amount of hydro power into the grid and simultaneously constraining the grid frequency. Results from SMPC indicate that there exists a trade-off between the amount of water flow through the turbine and the rate of change of the turbine's valve while constraining the grid frequency.

Keywords: microgrid, load and generation balance, intermittent injection, dispatchable hydro power, frequency stability, stochastic MPC

1 Introduction

1.1 Background

The demand for electricity generation from renewable energy is increasing because of oil insecurity, climatic concern, and the nuclear power debate. Renewable energy consists of intermittent and dispatchable energy sources. Intermittent generation from sources such as solar power, wind power, and tidal power exhibit fluctuating power production and creates an imbalance between generation and load. However, renewable dispatchable sources such as hydro power plants play a significant role in balancing out the variability caused by intermittent sources.

For instance, in a microgrid supplying electrical power to a common consumer load with generation from intermittent solar power and a dispatchable hydro power plant, injection of intermittent solar power into the grid creates a fluctuation in grid frequency. Assuming that he grid frequency must be maintained at the range of $(50 \pm 5\%)$ Hz, it is of interest to dispatch the required amount of hydro power into the grid for balancing out the load and the generation while maintaining the grid frequency in that range.

However, the required amount of hydro power production can not be dispatched instantaneously. In reality, changes in hydro power production are constrained by inertia in water and rotating mass, and the need to avoid wear and tear in actuators and other equipment. Furthermore, both solar power and consumer load are not known perfectly. The solar power and consumer load intermittency cause power imbalance into the grid and drifting in grid frequency. Improved performance can be achieved if the operation of the microgrid is optimized over some horizon with the added problem that intermittent power varies randomly into the future. Optimal management of dynamic systems over a future horizon with disturbances is often posed as an MPC problem.

1.2 Previous Work

An MPC approach had been applied for controlling water flow into the turbine in (Zhou, 2017). The use of MPC with consideration of dynamical model of hydro power systems is presented in (Munoz-Hernandez et al., 2012). Simulation results with different operating conditions and disturbances from previous work emphasize the use of an MPC-based approach over the optimal PI controllers (Avramiotis-Falireas et al., 2013; Bhagdev et al., 2019; Reigstad and Uhlen, 2020). In a recent study of (Pandey et al., 2021) stochastic analysis of deterministic MPC for a dynamical model of microgrid was performed. It is of interest to further extend the work of (Pandey et al., 2021) with SMPC with the addition of comparison between a PI controller and deterministic MPC.

1.3 Outline of the Paper

Section 2 provides a system description. The mathematical model of the microgrid is detailed in Section 3. The implementation of a deterministic MPC and a stochastic MPC is given in Section 4 and Section 5, respectively. Section 6 provides results and discussions. Conclusions and future work are outlined in Section 7.

2 System Description

Consider a microgrid as in Figure 1 a) operated at consumer load P_ℓ and supplied with intermittent solar power

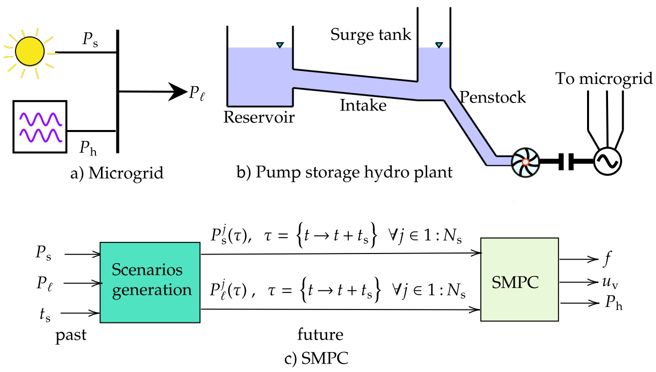

Figure 1. System description.

P_s. The difference between the intermittent generation and load is balanced with dispatchable hydro power P_h. Figure 1 b) shows the hydro power plant with reservoir, intake, surge tank, penstock, and turbine connected to the microgrid with an electrical generator. Figure 1 c) shows the N_s future scenarios generated in SMPC from the past data of P_s and P_ℓ. SMPC, as shown in the figure, keeps track of the constraint violation in grid frequency f for $50 \pm 5\%$ Hz and generates the turbine valve signal u_v and hydro power P_h dispatched into the grid based on the stochastic input from solar and consumer load.

3 Mathematical Model

3.1 Hydro Power Plant

The mathematical model for a hydro power plant shown in Figure 1 b) is taken from (Pandey et al., 2021) and given as

$$\frac{dh}{dt} = \frac{\dot{V}_s}{A_s} \tag{1}$$

$$\frac{d\dot{V}_s}{dt} = \frac{A_s}{\rho h}(p_n - p_a) - \frac{\pi D_s \dot{V}_s \mid \dot{V}_s \mid}{8A_s^2} f_{D,s} - gA_s \tag{2}$$

$$\frac{d\dot{V}_p}{dt} = \frac{A_p}{\rho L_p}(p_n - p_t) - \frac{\pi D_p \dot{V}_p \mid \dot{V}_p \mid}{8A_p^2} f_{D,p} + gA_p \frac{H_p}{L_p}, \tag{3}$$

with algebriac equations given by

$$p_t = p_a \left(1 + \left(\frac{\dot{V}_p}{C_v u_v}\right)^2\right) \tag{4}$$

$$\frac{d\dot{V}_i}{dt} = \frac{A_i}{\rho L_i}(p_a + \rho g H_r - p_n) - \frac{\pi D_i \dot{V}_i \mid \dot{V}_i \mid}{8A_i^2} f_{D,i} + gA_i \frac{H_i}{L_i} \tag{5}$$

$$\dot{V}_i = \dot{V}_s + \dot{V}_p \tag{6}$$

$$P_h = \eta_h (p_t - p_a) \dot{V}_p, \tag{7}$$

where the intake, the surge tank, and the penstock are subscripted with i, s and p, respectively. h is is the water level and $\dot{V}$ is the volumetric flow rate. Readers are requested to follow (Pandey et al., 2021) for notation.

3.2 Solar Power and Consumer Load

Solar power is calculated based on the solar irradiance k_I and given by

$$P_s = \eta_s A k_I \tag{8}$$

where η_s is the efficiency of a solar panel and A is the effective area of panels in the solar farm.

In contrast, the consumer load P_ℓ is modeled with the measurement data.

3.3 Grid

The grid is modeled with the *swing* equation given as

$$\frac{df}{dt} = \frac{P_m - P_e}{4\pi^2 f J} \tag{9}$$

where P_m is the mechanical power input into the microgrid with

$$P_m = P_h + P_s \tag{10}$$

and P_e is the electrical power load from the grid. The total inertia of the grid is represented by J.

3.4 Canonical Representation of the Model

The differential algebraic equations (DAEs) can be written in a canonical form of

$$\begin{aligned}
\frac{dx}{dt} &= f(x, z, u, w; \theta) \\
0 &= h(x, z, u, w; \theta) \\
y &= g(x, z, u, w, v; \theta),
\end{aligned}$$

where x, z, u, and θ represents system states, algebraic variables, inputs, and parameters respectively. w is the process disturbances and v is the measurement noise. For the microgrid shown in Figure 1 a) represented by mathematical equations from Eqs. (1) to (10), we have

$$\begin{aligned}
x &= (h, \dot{V}_s, \dot{V}_p, f) \\
z &= (p_t, p_n, \dot{V}_i, P_h, P_m) \\
u &= u_v \\
w &= P_s \\
\theta &= (H_j, L_j, D_j, A_j, H_r, \eta_h, C_v), \forall j = \{i, s, p\} \\
y &= P_e,
\end{aligned} \tag{11}$$

where the intermittent solar power P_s is considered as process disturbance and all states are assumed to be measured.

3.5 Case Study

It is of interest to see how a 5 MW hydro power plant can be used for balancing a 4 MW rated consumer load supplied with solar power. Table 1 lists specifications for power plants containing rated information, geometrical dimensions and efficiencies.

Table 1. Specifications of the power plants.

Parameters	Symbols	Values
Hydro power plant:		
Rated power	$P_{\mathrm{h}}^{\mathrm{r}}$	5 MW
Nominal head, discharge, valve signal	$H^{\mathrm{n}}, \dot{V}^{\mathrm{n}}, u_{\mathrm{v}}^{\mathrm{n}}$	$120\,\mathrm{m}, 4\,\mathrm{m}^3/\mathrm{s}, 0.95$120 m, 44 m^3/s,0.95
Height difference of reservoir, intake, surge tank and penstock	$H_{\mathrm{r}}, H_{\mathrm{i}}, H_{\mathrm{s}}, H_{\mathrm{p}}$	$20\,\mathrm{m}, 20\,\mathrm{m}, 50\,\mathrm{m}, 70\,\mathrm{m}$
Length of intake, surge tank and penstock	$L_{\mathrm{i}}, L_{\mathrm{s}}, L_{\mathrm{p}}$	$1000\,\mathrm{m}, 50\,\mathrm{m}, 80\,\mathrm{m}$
Diameter of intake, surge tank and penstock	$D_{\mathrm{i}}, D_{\mathrm{s}}, D_{\mathrm{p}}$	$3\,\mathrm{m}, 2\,\mathrm{m}, 2\,\mathrm{m}$
Hydraulic efficiency of hydro turbine	η_{h}	0.96
Inertia of turbine-rotor	J_{h}	$1 \cdot 10^3\,\mathrm{kgm}^2$
Solar power plant:		
Rated power and irradiance	$P_{\mathrm{s}}^{\mathrm{r}}, k_{\mathrm{I}}^{\mathrm{r}}$	$2.5\,\mathrm{MW}, 600\,\mathrm{W}/\mathrm{m}^2$
Effective area of total panels	A	$25000\,\mathrm{m}^2$
Solar panel efficiency	η_{s}	0.14

4 Deterministic MPC

A deterministic MPC can be formulated assuming known inputs from solar power P_{s} and consumer load P_{ℓ}. We want to formulate a setpoint tracking problem for P_{ℓ}.

4.1 Cost Function

The chosen cost function for formulating optimal control problem (OCP) for the deterministic MPC is taken from (Pandey et al., 2021) given as

$$\min_{u_k} \; J_{\mathrm{d}} = \sum_{k=1}^{N_{\mathrm{p}}} (y_k - r_k)^2 + p \cdot \Delta u_{k-1}^2 \tag{12}$$

$$\begin{aligned}
&\text{s.t.}\\
x_{k+1} &= f(x_k, z_k, u_k, w_k; \theta)\\
0 &= h(x_k, z_k, u_k, w_k; \theta)\\
y_k &= g(x_k, z_k, u_k, w_k, v_k; \theta)\\
x_\ell &\le x_k \le x_{\mathrm{h}}\\
u_\ell &\le u_k \le u_{\mathrm{h}}\\
\Delta u_\ell &\le \Delta u_k \le \Delta u_{\mathrm{h}},
\end{aligned}$$

where ℓ and h represents low and high bounds for states, inputs, and rate of change of inputs. N_{p} is the number of future samples in the prediction horizon where OCP is formulated. p is scalar weight for tuning the controller. r is the reference taken for consumer load power P_{ℓ}.

4.2 OCP Formulated in JuMP.jl

The internal structure of OCP is formulated in the Julia language[1] using JuMP.jl (Dunning et al., 2017), a Julia package for modeling mathematical optimization problems. JuMP provides an easy way of describing optimization problems containing linear and nonlinear constraints. JuMP also supports automatic differentiation (AD) using the package ForwardDiff.jl (Revels et al., 2016) which is

[1]https://julialang.org/

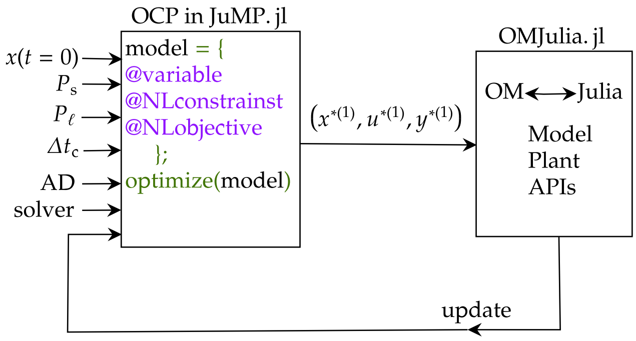

Figure 2. OCP formulated for deterministic MPC in JuMP.jl.

a most useful property rarely supported by other modeling languages. Several open-source solvers are available for solving models described in JuMP. Our choice of JuMP solver is Ipopt[2]. We have represented the plant by a Modelica model, and the controller model is implemented in Julia. These interact via OMJulia[3]. OMJulia is an OpenModelica-Julia interface providing application programming interfaces (APIs) for advanced model analysis in Julia.

Figure 2 shows the internal structure of OCP formulated in JuMP.jl for deterministic MPC. In the figure, $\left(x^{*(1)}, u^{*(1)}, y^{*(1)}\right)$ represents first optimal values of states, control inputs and control outputs from OCP. We have assumed that all the states are known. These optimal control inputs are then applied to the emulated real plant developed in OpenModelica[4]. Similarly, both the optimal states and the control inputs are applied to the mathematical model. The states, inputs, and outputs are accessed through OMJulia APIs for further iteration.

[2]https://github.com/jump-dev/Ipopt.jl
[3]https://github.com/OpenModelica/OMJulia.jl
[4]https://www.openmodelica.org/

5 Stochastic MPC

Several stochastic MPC algorithms can be used for handling uncertainty in the system (Camacho and Bordons, 2016). A comparative study on stochastic MPC is given in (González et al., 2020). Comparison of the different stochastic MPC algorithms are out of the scope of this paper. In this paper, more focus is on the implementation of the dynamic formulation of the microgrid with stochastic solar power and load power. We have chosen multi-objective optimization (MOO) based stochastic MPC with similar formulation from the previous work our institution (Menchacatorre et al., 2020) as it is easier to formulate and have a quick analysis. In MOO-based stochastic MPC, we create scenarios of random disturbances; and in our case the random disturbances are P_{s} and P_{ℓ}. Each scenario is then assigned with an objective function or a constraint. When each of the objective functions is summed together by assigning weights to each of the objectives, a single objective function is created which is called a weighted-sum MOO.

5.1 Cost Function

The MOO based cost function for N_{s} number of stochastic scenarios for P_{s} and P_{ℓ} is given as

$$\min_{u_k} \; J_{\text{s}} = \sum_{s=1}^{N_{\text{s}}} \left(\sum_{k=1}^{N_{\text{p}}} (y_k^s - r_k^s)^2 + p \cdot \Delta u_{k-1}^2 \right) \tag{13}$$

$$\begin{aligned} \text{s.t.} \quad & \\ x_{k+1}^s &= f\left(x_k^s, z_k^s, u_k, w_k^s; \theta\right) \\ 0 &= h\left(x_k^s, z_k^s, u_k, w_k^s; \theta\right) \\ y_k &= g\left(x_k^s, z_k^s, u_k, w_k^s, v_k^s; \theta\right) \\ x_\ell &\leq x_k^s \leq x_{\text{h}} \\ u_\ell &\leq u_k \leq u_{\text{h}} \\ \Delta u_\ell &\leq \Delta u_k \leq \Delta u_{\text{h}}, \end{aligned}$$

where we have considered each of the scenarios to be equally important; thus the total objective is formulated summing objective function of each of the scenarios. This cost function is used for formulating OCP for stochastic MPC. A stochastic MPC is formulated by solving OCP for each iteration considering N_{p} number of future samples in the prediction horizon.

5.2 Stochastic Scenarios for P_{s} and P_{ℓ}

Real measurement for solar irradiance is taken for Kjølnes Ring 56, Campus Porsgrunn, University of South-Eastern Norway, 9.6714 longitudes and 59.13814 latitudes from www.solcast.com. The measurement data is updated at every 5 min throughout the day. The real measurement for consumer load is taken for monthly hourly averaged load for Norway from ENTOS-E[5]. The magnitude of measurement data for electrical demand is modified as per our case study with a microgrid with a power capacity of 5 MW keeping the load dynamics preserved in hourly data. Furthermore, the hourly sampled data is interpolated for creating consumer load with a sampling of 5 min.

[5]https://www.entsoe.eu/data/power-stats/

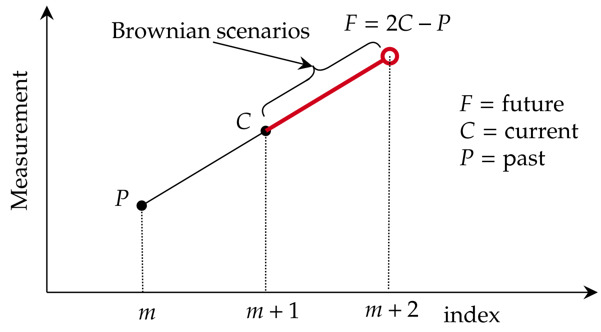

Figure 3. Scenarios generation based on the past measurement.

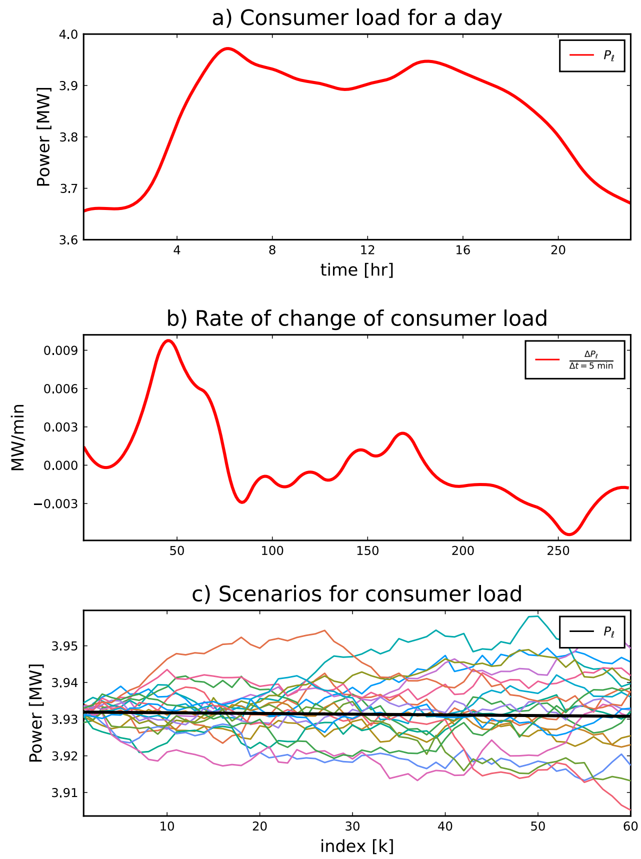

Figure 4. Scenarios generation for P_{ℓ}.

Between each of the measurements, scenarios are generated using a stochastic evolution equation considering a *Brownian* motion[6]. The stochastic evolution equation based on the Brownian motion is used as a *generatrix* and a straight line between the two measurements is used as a *directrix*.

Figure 3 shows the method for generating future scenarios based on the past and current measurements sampled

[6]https://en.wikipedia.org/wiki/Brownian_motion

DOI: 10.3384/ecp21185196

at 5 min. In the figure, the future measurement F is predicted from past measurement P and current measurement C. Assuming measurement P, C and F are co-linear we have

$$\frac{F-C}{(m+2)-(m+1)} = \frac{C-P}{(m+1)-m},$$

which gives

$$F = 2C - P.$$

The stochastic scenarios are then creating using Brownian motion between current measurement C and future prediction F.

Figure 4 a) shows consumer load on a typical day with measurement data taken at 5 min. Figure 4 b) shows rate of change of consumer load for $\Delta t \to 5$ min where the data points within a day consist of 288 data points and represented as $P_\ell = \{P_\ell[m]\ \forall m \in 1:288\}$. The figure shows that the bound for $\frac{\Delta P_\ell}{\Delta t = 5\,\text{min}}$ lies in $[-0.002, 0.009]$. The standard deviation for Brownian motion for creating scenarios is then set to > 0.011. Figure 4 c) shows the future predicted P_ℓ from the past measurement P and current measurement C considering co-linear existence between P, C and F as shown in Figure 3. For P_ℓ in Figure 4 b) we have assumed that $P = P_\ell[99]$, $C = P_\ell[100]$ and $F = P_\ell[101]$. Figure 4 c) shows 20 scenarios generated using Brownian motion. The same procedure is applied for

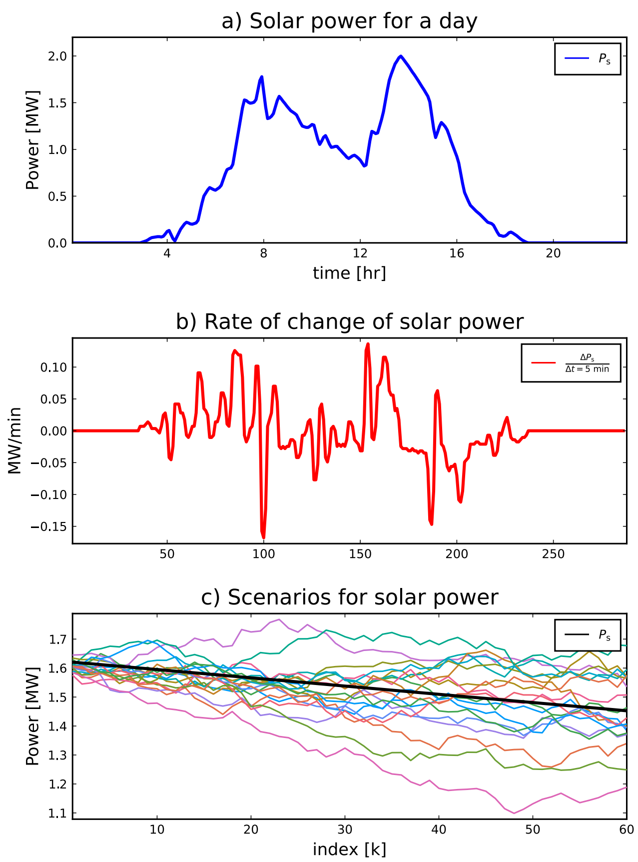

Figure 5. Scenarios generation for P_s.

predicting P_s as shown in Figure 5 where the standard deviation for Brownian motion is set to > 0.3 which is comparatively larger than in case of consumer load scenarios generation. The standard deviation in scenarios is much higher in case of prediction of P_s because of the clouds. A more rigorous algorithm for predicting scenarios of P_s depends on the information of clouds injected into the prediction algorithms. Since we have only focused on formulation of stochastic MPC, we neglected the part of considering cloud information while generating scenarios for P_s.

5.3 Stochastic OCP

We have considered the prediction horizon of $N_p = 10$. The discretization time of the controller for SMPC is chosen to be $\Delta t = 5$ s based on our previous work for a microgrid with around 5 MW (Pandey et al., 2021). For moving along the stochastic prediction horizon of P_s and P_ℓ, the states and the outputs are updated taking the mean of the first value of each of the scenarios of states and outputs from the stochastic OCP.

6 Results and Discussions

6.1 Deterministic MPC

Figure 6 shows setpoint tracking formulation of consumer load P_ℓ using both deterministic MPC and a PI controller. The MPC is characterized by tuning parameter $p = 0.1$, $N_p = 5$ and $\Delta t = 1$ s. Similarly, the PI controller is characterized with $K_p = 0.05$ and $T_i = 3$ s. The initial tuning of the PI controller is based on the SIMC method (Skogestad, 2001) and the final tuning was performed manually. The setpoint tracking of P_ℓ using the PI controller is performed using OpenHPL in OpenModelica while the MPC is formulated as in Figure 2 in conjunction with real plant considering from OpenHPL and the control model is formulated in Julia. The control model is discretized using Euler discretization.

Figure 6 a) shows the setpoint tracking using both MPC and PI controller. A step change in P_ℓ is performed at time $=25$ s while a step change in P_s is performed at time $=50$ s. Figure 6 b) shows the hydro power dispatched into the grid from both the MPC and the PI controller. The control input, turbine valve signal u_v, for controlling the flow rate through the penstock for balancing the load and the generation is shown in Figure 6 c). Similarly, Figure 6 d) shows the grid frequency f of the microgrid. In Figure 6 c) we see that u_v in case of the MPC is smoother and less fluctuating than u_v in case of the PI controller. Furthermore, since an MPC works based on the future horizon, in Figure 6 c) the turbine valve signal u_v in case of the MPC is increased from 0.4 to 0.6 at time ≈ 23 s keeping the constraint in grid frequency for $f \approx 50$ Hz (small deviation not shown in the figure). Contrary to the performance of the MPC, from the figure the turbine valve signal is increased exactly at time $=25$ s while the grid frequency f fluctuates from 50 Hz to 47.5 Hz. The PI controller is able to regain

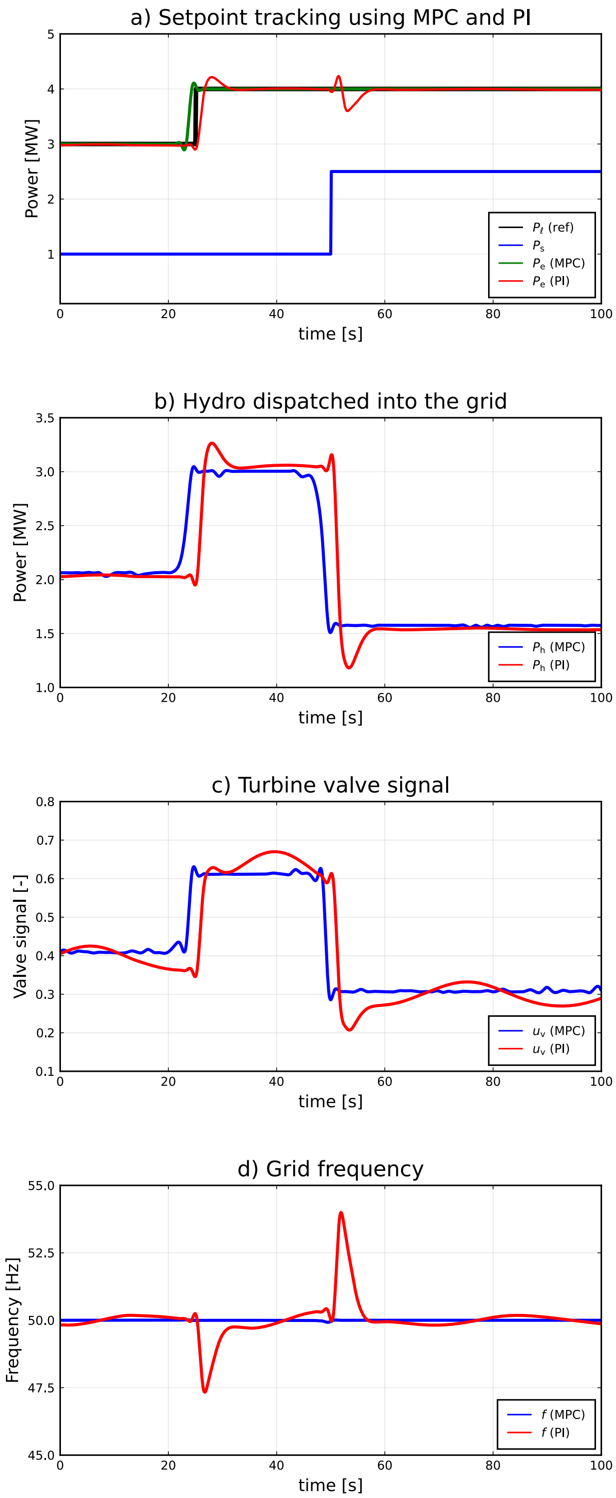

Figure 6. Setpoint tracking using deterministic MPC and PI controller.

the grid frequency around 50 Hz after ≈ 5 s. Similar, results can be seen in the case of hydro power P_h dispatched into the grid and the electrical power P_e. The similar dynamics of P_ℓ and P_e with u_v in case of both the MPC and the PI controller can be related from Equations (4), (7), and (9). Overall, the performance of the MPC is better than that of the PI controller.

6.2 Stochastic MPC

Figure 7 shows the tracking of the future predicted consumer load P_ℓ based on the future prediction of solar power P_s into the grid where both future predicted P_ℓ and P_s are taken from Section 5.2. The MOO based stochastic MPC is characterized by $N_p = 10$, $N_s = 20$, $p = 0.1$ and $\Delta t = 5\,\mathrm{s}$. The next scenarios for P_ℓ and P_s are updated every 5 min = 300 s using the current measurement C and the past measurement P as shown in Figure 3.

Figure 7 a) shows the turbine valve signal u_v generated for each of the scenarios considering a deterministic MPC. The results for u_v from the deterministic MPC for each of the scenarios are considered as an ensemble of trajectories for u_v. In the figure, u_v (MOO) is the results from the stochastic MPC based on MOO in tandem with the ensemble of results from deterministic MPC for each of the scenarios. The fluctuation in the grid frequency is negligible as in the range of $1 \cdot 10^{-4}$ rad/s for both the deterministic and stochastic case as shown in Figure 7 f). Figure 7 b), c), d) and e) show the results from both the deterministic and stochastic case for hydro dispatched P_h, electrical power into the grid P_e, flowrate into the penstock $\dot{V}_p$, and the water mass oscillation inside the surge tank h, respectively.

7 Conclusions and Future Work

In this paper formulation of a deterministic and a stochastic MPC is performed for a microgrid supplied with intermittent solar power and dispatchable hydro power for constraining the grid frequency at $f = 50$ Hz. A deterministic MPC is compared with a PI controller. Furthermore, for the stochastic MPC, the scenarios for solar power and the consumer load are predicted using Brownian motion using past and current measurement data. A MOO-based stochastic MPC is implemented.

Results indicate that the deterministic MPC performs better for constraining the grid frequency of the microgrid at $f = 50$ Hz than to the PI controller. The stochastic MPC based on MOO shows better result than deterministic MPC while constraining the grid frequency.

Future work includes the implementation of stochastic MPC with scenario generation for solar power with the inclusion of cloud factors.

References

Iason Avramiotis-Falireas, Athanasios Troupakis, Farzaneh Abbaspourtorbati, and Marek Zima. An MPC strategy for automatic generation control with consideration of deterministic power imbalances. In *2013 IREP Symposium Bulk Power System Dynamics and Control-IX Optimization, Security and Control of the Emerging Power Grid*, pages 1–8. IEEE, 2013. doi:10.1109/IREP.2013.6629359.

Dishant Bhagdev, Rajasi Mandal, and Kalyan Chatterjee. Study and application of mpc for agc of two area interconnected thermal-hydro-wind system. In *2019 Innova-*

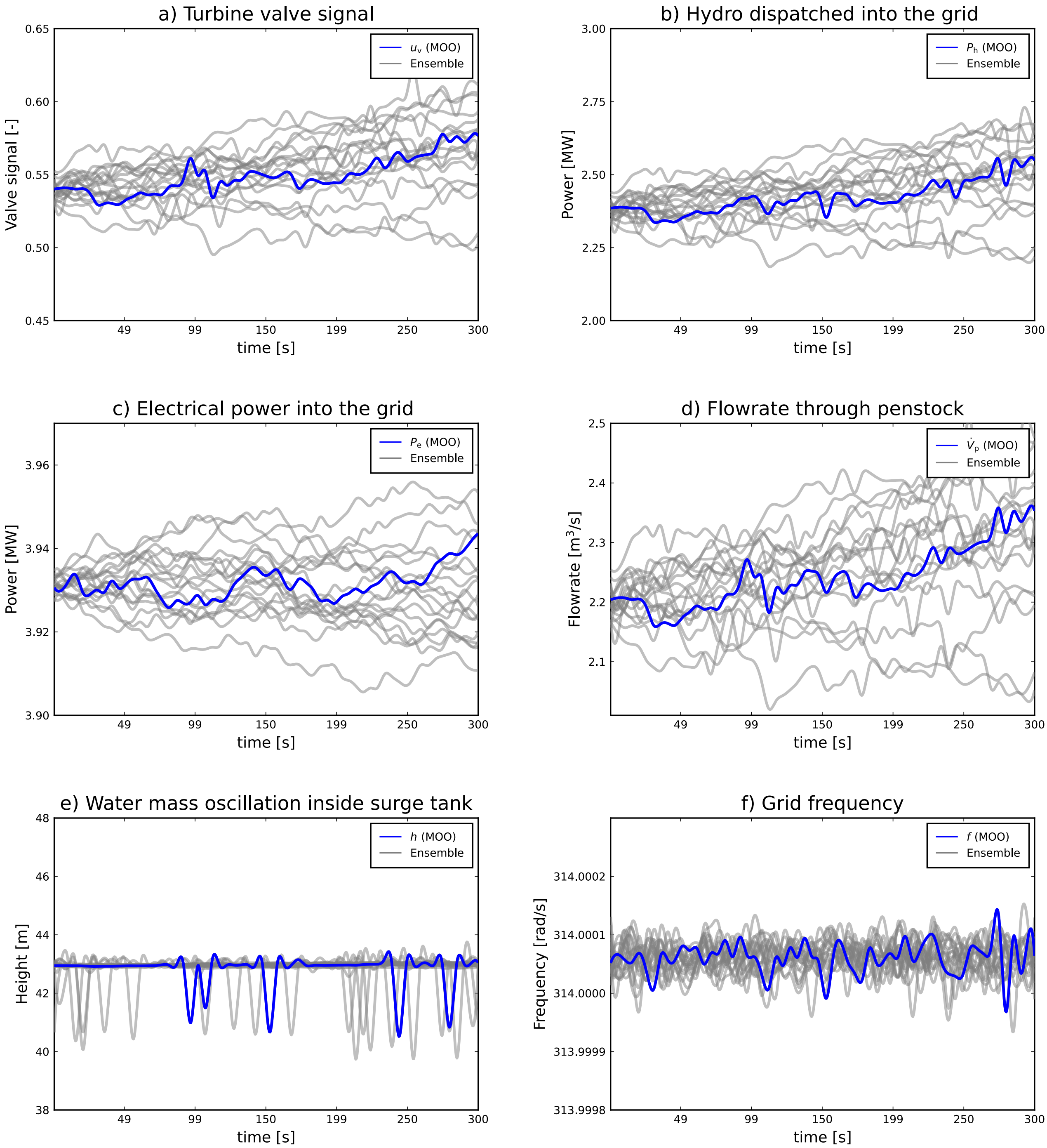

Figure 7. Deterministic and stochastic comparison for scenarios generated for P_s and P_ℓ in Section 5.2.

tions in Power and Advanced Computing Technologies (i-PACT), volume 1, pages 1–6. IEEE, 2019. doi:10.1109/i-PACT44901.2019.8960124.

Eduardo F Camacho and Carlos Bordons. *Model predictive control: Classical, robust and stochastic*. Springer International Publishing, 2016.

Iain Dunning, Joey Huchette, and Miles Lubin. Jump: A modeling language for mathematical optimization. *SIAM Review*, 59(2):295–320, 2017. doi:10.1137/15M1020575.

Edwin González, Javier Sanchis, Sergio García-Nieto, and José Salcedo. A comparative study of stochastic model predictive controllers. *Electronics*, 9(12):2078, 2020. doi:10.3390/electronics9122078.

Itsaso Menchacatorre, Roshan Sharma, Beathe Furenes, and Bernt Lie. Flood Management of Lake Toke: MPC Operation under Uncertainty. In *Proceedings of The 60th SIMS Conference on Simulation and Modelling SIMS 2019, August 12-16, Västerås, Sweden*, number 170, pages 9–16. Linköping University Electronic Press, 2020. doi:10.3384/ecp201709.

German Ardul Munoz-Hernandez, Dewi Ieuan Jones, et al. *Modelling and controlling hydropower plants*. Springer Science & Business Media, 2012. doi:10.1007/978-1-4471-2291-3.

Madhusudhan Pandey, Dietmar Winkler, Roshan Sharma, and Bernt Lie. Using MPC to Balance Intermittent Wind and Solar Power with Hydro Power in Microgrids. *Energies*, 14(4): 874, 2021. doi:10.3390/en14040874.

Tor Inge Reigstad and Kjetil Uhlen. Optimized control of variable speed hydropower for provision of fast frequency reserves. *Electric Power Systems Research*, 189:106668, 2020. doi:10.1016/j.epsr.2020.106668.

J. Revels, M. Lubin, and T. Papamarkou. Forward-mode automatic differentiation in Julia. *arXiv:1607.07892 [cs.MS]*, 2016. URL `https://arxiv.org/abs/1607.07892`.

Sigurd Skogestad. Probably the best simple pid tuning rules in the world. In *AIChE Annual Meeting, Reno, Nevada*, volume 77, 2001. URL `https://folk.ntnu.no/skoge/publications/2003/tuningPID/more/old-original_rejected_version_from_July01/tuningpaper.pdf`.

Wenjing Zhou. Modeling, Control and Optimization of a Hydropower Plant. 2017. Doctoral dissertations at the University College of Southeast Norway;33.